

Article

Sucrose Hydrolysis in a Bespoke Capillary Wall-Coated Microreactor

Filipe Carvalho ¹, Marco P. C. Marques ² and Pedro Fernandes ^{1,3,*}

¹ Department of Bioengineering and IBB—Institute for Bioengineering and Biosciences, Instituto Superior Técnico, Universidade de Lisboa, Av. Rovisco Pais, 1049-001 Lisboa, Portugal; filipe.ramos.carvalho@tecnico.ulisboa.pt

² Department of Biochemical Engineering, University College London, Bernard Katz Building, Gordon Street, London WC1H 0AH, UK; marco.marques@ucl.ac.uk

³ Faculty of Engineering, Universidade Lusófona de Humanidades e Tecnologias, Av. Campo Grande 376, 1749-024 Lisboa, Portugal

* Correspondence: pedro.fernandes@tecnico.ulisboa.pt; Tel.: +351-21-8419594

Academic Editor: David D. Boehr

Received: 14 November 2016; Accepted: 24 January 2017; Published: 27 January 2017

Abstract: Microscale technology has been increasingly used in chemical synthesis up to production scale, but in biocatalysis the implementation has been proceeding at a slower pace. In this work, the design of a low cost and versatile continuous flow enzyme microreactor is described that illustrates the potential of microfluidic reactors for both the development and characterization of biocatalytic processes. The core structure of the developed reactor consists of an array of capillaries with 450 μm of inner diameter with their inner surface functionalized with (3-aminopropyl)triethoxysilane (APTES) and glutaraldehyde where *Saccharomyces cerevisiae* invertase was covalently bound. The production of invert sugar syrup through enzymatic sucrose hydrolysis was used as model system. Once the microreactor assembly reproducibility and the immobilized enzyme behavior were established, the evaluation of the immobilized enzyme kinetic parameters was carried out at flow rates ranging from 20.8 to 219.0 $\mu\text{L}\cdot\text{min}^{-1}$ and substrate concentrations within 2.0%–10.0% (*w/v*). Despite the impact of immobilization on the kinetic parameters, viz. $K_{m(\text{app})}$ was increased two fold and K_{cat} showed a 14-fold decrease when compared to solution phase invertase, the immobilization proved highly robust. For a mean residence time of 48.8 min, full conversion of 5.0% (*w/v*) sucrose was observed over 20 days.

Keywords: microchannel reactor; biocatalysis; enzyme immobilization; sucrose hydrolysis; continuous processing

1. Introduction

The use of microscale technology in chemical synthesis, biomedical devices, analytics and point of care diagnostic systems has long been established and continuous to grow at great pace [1–6]. This fact is due to the high set of benefits that arise from the use of microscale platforms both at the product development and production stages. The high throughput required at the different stages of process development is easily achieved due to the high level of parallelization obtained with microscale platforms resulting in a faster transfer from the development stage into market; when compared with conventional platforms, miniaturized devices present a higher surface to volume ratio which significantly enhances heat and mass transfer due to the short diffusion paths; and solutions typically flow in laminar regime resulting in increased spatial and temporal reaction control; the energy requirements and reagent consumption decrease considerably, contributing to an overall reduction of the costs and environmental impact; transfer from bench scale to production scale may be achieved by simply numbering up rather than scaling up [7–10].

Microreactors have already become a key component in chemical synthesis, yet its potential in biocatalysis, with the exception to the microwell format in process development, has not been fully capitalized, although their application in some relevant reaction systems supports the validity of the approach [11]. This is partly related to the ability of biocatalysts to operate under mild conditions where the generation of toxic and/or explosive compounds does not occur and therefore safety issues are usually not relevant. Nonetheless, on the quest for high performance/sustainable manufacturing technologies, the combination of biocatalysis and microscale technology display a wide set of appealing features and new opportunities worth to embrace, such as the separation of unstable intermediates from the reaction media [7,9,10,12].

Continuous flow processing offers substantial benefits when compared to standard batch operation mode, especially regarding the overall reduction of operation costs, the possibility to maintain product quality standards along with the operation time, and the implementation of coupled reaction pathways. In order to further reduce the operation costs and increase biocatalyst productivity ($kg_{product}/kg_{biocatalyst}$), biocatalysts are preferentially used in the immobilized form [13–17]. Numerous methods have been developed to immobilize biocatalysts in conventional reaction systems [18] and the same methodologies may be applied in microscale platforms. Nonetheless, in microfluidic devices, special attention has been given to both: the immobilization of biocatalysts onto particulate supports and their loading on a packed bed reactor configuration [13,14,19,20]; and to the immobilization of the biocatalyst on the inner surface of microchannels, so called wall-coated microreactors [15–17,21,22]. While back pressure issues and the complex liquid flow pattern observed on packed bed reactors are clear drawbacks that can limit scale-up, lower volumetric productivity may result of the use of wall-coated microreactors due to the lower reactive surface area available for reaction [17]. Nonetheless, the latter can be easily tackled by increasing the number of channels of the biocatalytic platform, increasing in this way the overall activity density.

The present work is within the framework of the development of biocatalytic continuous flow processes in microfluidic environments. A low cost and easy to assemble and disseminate microchannel reactor constituted by an array of capillaries was developed. To the authors knowledge, this specific configuration, reminiscent of a hollow fiber reactor that can be assembled in a reproducible manner using commonly available materials and methodologies, has not been disclosed for enzymatic microreactors. The inner capillary wall was functionalized firstly by the introduction of amine groups via silanization with 3-aminopropyltriethoxysilane (APTES) followed by the introduction of the bi-functional cross-linking reagent glutaraldehyde where the biocatalyst was covalently bound. Covalent binding of the enzyme to the support is a well-established method, often used when avoiding enzyme leakage from the support is a primary concern [23]. Within this particular approach for enzyme immobilization, glutaraldehyde is one of the most disseminated cross-linking agents to bind the enzyme to the support, mostly through the formation of both Schiff bases and Michael-type additions [24,25]. Accordingly, it has also been used when enzymatic microreactors are addressed, in monolith [26], packed bed [13,20,27] and wall-coated configurations [16,17,21]. The developed microreactor assembly methodology proved to be highly reproducible, which led to the establishment of optimal operational conditions under varying conditions of pH and temperature. Robustness was assessed in continuous mode of operation by the study of the effect of substrate concentration and flow rates on the product yield, the evaluation of kinetic parameters under flow conditions and analysis of mass transfer effects. Long-term operational stability in continuous mode was assessed throughout a 30 days period.

Due to both the extensive data available in the literature [28–33] and commercial relevance [34], the biocatalytic system used on the present work was the hydrolysis of sucrose catalyzed by *Saccharomyces cerevisiae* invertase yielding an equimolar mixture of glucose and fructose (invert sugars).

2. Results and Discussion

2.1. Microchannel Reactor Assembly and Enzyme Immobilization Reproducibility

The present study aimed to develop and characterize an easy to assemble and low cost microchannel reactor. In Figure 1, the activity profiles of sucrose hydrolysis catalyzed by immobilized invertase in three microchannel reactor replicas are presented. Full conversion of a 5.0% (*w/v*) sucrose solution was achieved on all reactor replicas after roughly 6 h of reaction. Moreover, the conversion profiles observed are similar. Therefore, reactor assembly and capillary inner wall enzyme immobilization protocol proved to be highly reproducible. The microreactor was operated as a differential reactor, in full recirculation mode. Under the chosen mode of operation, corresponding to a residence time of approximately 7 s, conversion with each pass through the reactor is minimal, but with the multiple passes conversion increases steadily with time. Given the prolonged time span, the differential recirculation reactor behaves as a batch reactor. Still, in the former, the reaction only takes place in a small fraction of reaction medium, whereas, in the later, it takes place in all of the reaction medium.

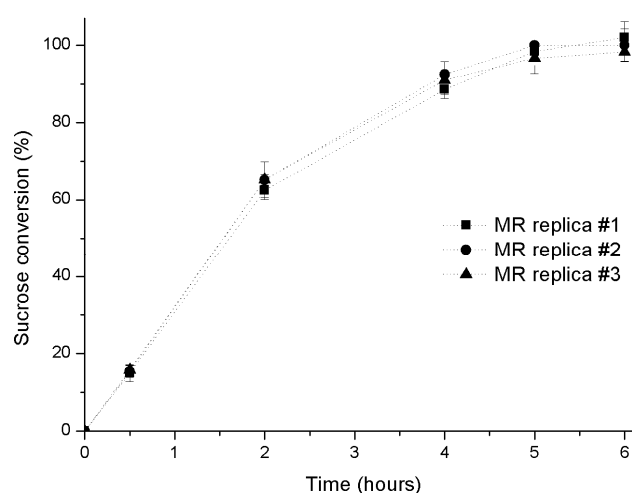


Figure 1. Conversion profiles of sucrose hydrolysis catalyzed by immobilized invertase in three microchannel reactor replicas. Five milliliters of a 5.0% (*w/v*) sucrose solutions pH 4.5 were fed to the microchannel reactors in recirculation mode at a flow rate of $3.50 \text{ mL}\cdot\text{min}^{-1}$. Runs were performed at $50 \text{ }^\circ\text{C}$ in triplicates. Error bars represent standard deviation.

2.2. Effect of pH and Temperature on the Catalytic Activity of the Free and Immobilized Invertase

Both temperature and pH of the reaction media strongly influence the catalytic performance of enzymes and the corresponding activity profiles have been widely reported to change as the outcome of immobilization [13,28,35–37]. The temperature and pH activity profiles for the hydrolysis of sucrose with free and immobilized invertase are presented in Figure 2. Regarding pH, the free invertase presented the highest catalytic activity at pH 5.0 and retained roughly 56% and 83% of activity at pH values of 3 and 6, respectively (Figure 2a); whereas the immobilized enzyme showed to be more active at lower pH values, presenting the highest activity at pH 4.5 and maintaining approximately 70% of activity at pH 3.0 and 71% at pH 6 (Figure 2a). Invertase immobilization resulted in an increased endurance towards higher temperatures; the optimal temperature for the immobilized form was observed to be $60 \text{ }^\circ\text{C}$, whereas the free form presented higher catalytic activity at $55 \text{ }^\circ\text{C}$ (Figure 2b).

Similar effect of pH and temperature has already been reported for the immobilization of laccase [38,39] and invertase [13] onto aminated silicone dioxide based carriers using glutaraldehyde as crosslinking agent. These catalytic behavior deviations upon immobilization are usually assigned to: (i) the stabilization of the tertiary structure of the enzyme that result from the attachment to the

immobilization carrier, leading to a decrease in structure flexibility [40]; and (ii) alterations of enzyme microenvironment that improves the retention of activity at extreme pH values [41].

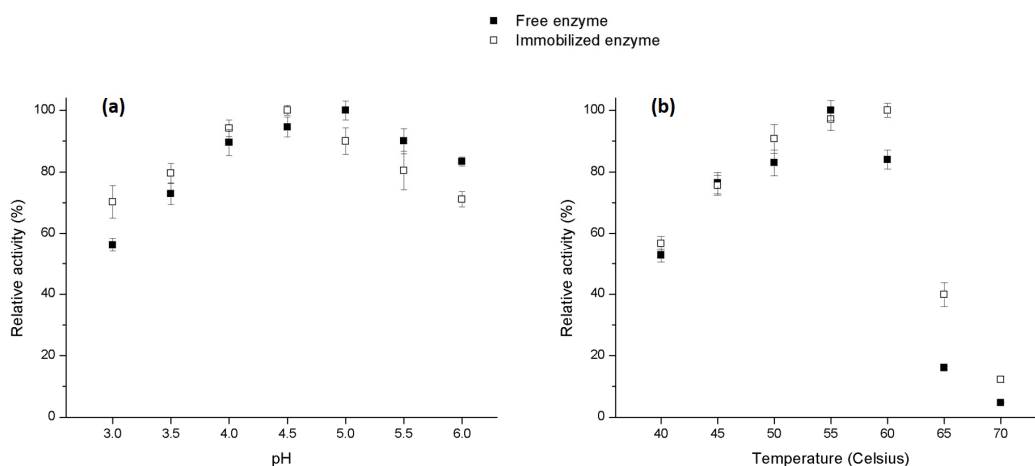


Figure 2. Effect of pH (a); and temperature (b) on the hydrolytic activity of the free (closed squares) and immobilized (open squares) enzyme. pH was evaluated in the range of 3.0 to 6.0, at a temperature of 50 °C and temperature was assessed at temperatures ranging from 40 to 70 °C at pH 4.5. Experiments were performed in triplicates, at a flow rate of 3.5 mL·min⁻¹, and error bars represent the standard deviation.

2.3. Operational Stability in Recirculation Mode

Heterogeneous biocatalysis renders the possibility to perform a reaction in continuous mode without constant supply of biocatalyst while reducing the complexity and costs associated with the downstream process. Nonetheless, the immobilized biocatalyst must also present adequate operational stability that enables the operation for extended periods of time or in consecutive reaction cycles. The lack of operational stability seriously compromises the effort to implement biocatalytic processes at the production scale. In order to have some insight on the retention of catalytic activity and assess enzyme leakage under operational conditions, some runs were performed in full recirculation mode.

Along four consecutive reaction cycles the invertase immobilized on the inner wall of the capillaries was able to catalyze the full conversion of a 5.0% (*w/v*) sucrose solution in roughly 6 h (Figure 3).

Moreover, with the exception from the first reaction cycle, where higher reaction rate was observed, similar reaction rates were detected (Figure 3). The reaction rate decrease from the first to the second cycle is assigned to the leakage of physically adsorbed enzyme that has not been properly washed out on the last step of the assembly of the biocatalytic platform. This fact was confirmed by the detection of trace amounts of protein in solution at the end of the first reaction cycle; nonetheless, no protein leakage was detected on the following cycles (data not shown). Negligible, if any, enzyme leakage of the support upon cross-linking with glutaraldehyde was also reported in other works [25]

The developed microchannel reactor was successfully employed for the rapid evaluation of the operation stability of the immobilized biocatalyst. The results revealed that the immobilization strategy used is highly robust. Therefore, further characterization was carried out in continuous flow operation.

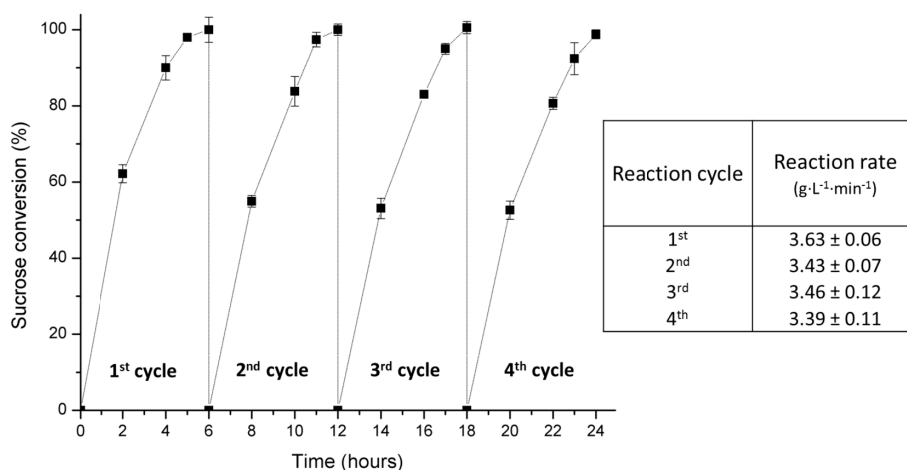


Figure 3. Conversion profiles and corresponding reaction rates of the immobilized invertase. Data represent four consecutive reaction cycles. Five milliliters sucrose solution (5.0% (*w/v*) at pH 4.5) was fed to the microchannel reactor in recirculation mode at a flow rate of 3.50 mL·min⁻¹. Runs were performed at 50 °C. At the beginning of each cycle, fresh substrate solution was added. Experiments were performed in triplicates and error bars represent the standard deviation.

2.4. Immobilized Invertase Kinetic Parameters in Continuous Flow

Enzyme immobilization may be associated with several phenomena that strongly influence the enzyme kinetic parameters, viz. steric hindrance, deactivation, presence of charged groups on the support, support hydrophilicity/hydrophobicity and mass transfer limitations [13,18,42–44]. Frequently, enzyme kinetics is evaluated in transient or pre-steady state conditions by stopped-flow or chemical quench-flow methods [42,45,46]. However, when the development and characterization of continuous flow reaction system is aimed, such methodologies fail to achieve adequate kinetic evaluation because flow rates affect the rate of diffusion of substrate into the surroundings of the enzyme [13,15,47,48]. In order to overcome this issue, Lilly et al. introduced a model that allows evaluating the kinetic parameter of a biocatalyst in continuous mode [48]. Additionally, this model assesses the impact of flow rates on the mass transfer effects. The model is an adaptation of the standard Michaelis–Menten enzyme kinetic model and was originally developed for packed bed, assuming plug flow and negligible inhibition. Nonetheless, it has also been applied for the evaluation of the kinetic parameters of enzymes immobilized on the inner walls of capillaries assuming negligible residence time distribution (RTD) broadening due to the occurrence of axial dispersion and to the parabolic flow profile [15,17,49]. In fact, according to Commenge et al., microchannel reactors will likely exhibit reduced RTD dispersion when compared to equivalent packed bed reactors [50]. This fact can be justified by the hydrodynamic singularities encountered in packed beds, namely the successive constriction and broadening of the fluid volume and the bed tortuosity. Furthermore, when enzymatic reactor modeling is envisaged, it has been observed by Carrara et al. that accurate prediction of reactor behavior is more dependent on the use of the correct kinetic reaction mechanism than the characteristics assumed of the flow distribution [51]. Accordingly, in the present work, the Lilly–Hornby model has been employed to evaluate the immobilized invertase kinetic parameters in continuous flow. The model is summarized by the following equation:

$$f[A_0] = K_{m(app)} \ln(1 - f) + \frac{C}{Q} \quad (1)$$

where f is the fraction of substrate converted to product during the reaction, $[A_0]$ the initial substrate concentration, $K_{m(app)}$ is the apparent Michaelis–Menten constant, C is the reaction capacity of the microreactor ($C = V_{max} \times Volume_{void}$) and Q is the flow rate of the substrate.

The evaluation of the immobilized enzyme kinetic parameters was carried out at flow rates ranging from 20.8 to 219.0 $\mu\text{L}\cdot\text{min}^{-1}$ (corresponding to a mean residence times in the range of 1.78 to 18.75 min) and substrate concentrations in the range of 2.0%–10.0% (w/v). The reducing sugar concentration was measured at the outlet of the microchannel reactor. The results for the conversion of sucrose to reducing sugars obtained in the aforementioned conditions are presented in Figures 4 and 5.

Conversion profiles showed the expected trend, already observed in previous work [13], where conversion yields increased proportionally to the feed concentration (Figure 4a) and residence time (Figure 4b). The obtained data were used to plot the Lilly–Hornby model, where $f[A_0]$ against $\ln(1 - f)$ results in a straight line with a slope equal to $K_{m(app)}$ (Figure 5a). Over the tested range of flow rates, the slopes of the fitted lines did not present statistically significant differences (Figure 5b), showing that the $K_{m(app)}$ value is not flow rate dependent. According to the Lilly–Hornby model, such behavior is justified by the absence of substrate diffusional limitations. The same trend has been reported by Vodopivec et al., while studying the kinetic behavior of lactate dehydrogenase immobilized on a monolith reactor [52]. Furthermore, several authors observed that when $K_{m(app)}$ is flow rate dependent, an increase in the flow rate usually leads to a decrease on $K_{m(app)}$ [13,14,17,48]. This is credited to the fact that the transport rate of the substrate through the diffusion layer surrounding the immobilized enzyme is inversely proportional to its thickness; and the diffusion layer thickness is proportional to the flow rate [48].

Accordingly, increasing flow rates will result in a less pronounced diffusional effect, eventually until a point where mass transfer resistances are absent and $K_{m(app)}$ values level off [13,14]. On the other hand, $K_{m(app)}$ values have also been reported to increase with increasing flow rates as a result of the presence of strong mass transfer effects associated with the use of fast enzymatic reactions [15,53].

$K_{m(app)}$ revealed a two fold increase when compared to the values obtained for the free enzyme, shifting from 14.6 to 28.2 $\text{g}\cdot\text{L}^{-1}$. The corresponding K_{cat} of the immobilized invertase under continuous flow (mass of invertase in the capillary microreactor = 3.06×10^{-5} g) revealed to be roughly 14 times less than that observed for the free form, 2.5 and 36.6 s^{-1} respectively. From the comparison of the kinetic parameters it is concluded that the immobilization procedure both decreased the affinity of the enzyme towards the substrate and the catalytic performance. These observations are well known from the literature and when no diffusional limitations are detected are often assigned to: (i) several events that may occur during the immobilization procedure, viz. alteration of enzyme conformation, imperfect immobilization chemistry, enzyme deactivation and steric hindrance [45,47,52,54]; and/or (ii) to the nature of the immobilization support, viz. presence of charged groups and hydrophilicity/hydrophobicity [44]. Moreover, when using amorphous materials as immobilization carrier combined with protocols involving the formation of self-assembly monolayers, non-uniform distribution and formation of enzyme aggregates is likely to occur often as the result of molecular polymerization phenomena and surface nucleation. These events will also affect the apparent kinetic parameters because substrate may not be available at the same extent to every immobilized enzyme molecule. In the present case, the results obtained seem to rule out mass transfer limitations, the increase in $K_{m(app)}$ indicating a decrease in enzyme–substrate complexation rate as compared to the free enzyme, could be ascribed to conformational changes due to the binding of the enzyme to the support. This leads to a less favorable configuration of the active site [45,55,56]. Besides conformational changes, the decrease in K_{cat} can also be ascribed to steric hindrances [13,55–57].

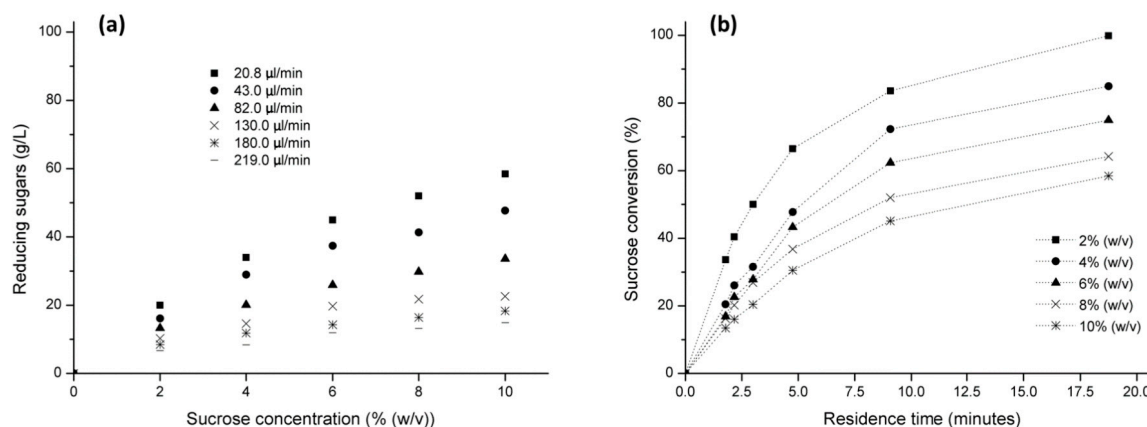


Figure 4. Bioconversion in the microchannel reactor using flow rates in the range of 20.8 to 219.0 $\mu\text{L}\cdot\text{min}^{-1}$ (a); and substrate concentrations ranging from 2.0% to 10.0% (w/v) (b).

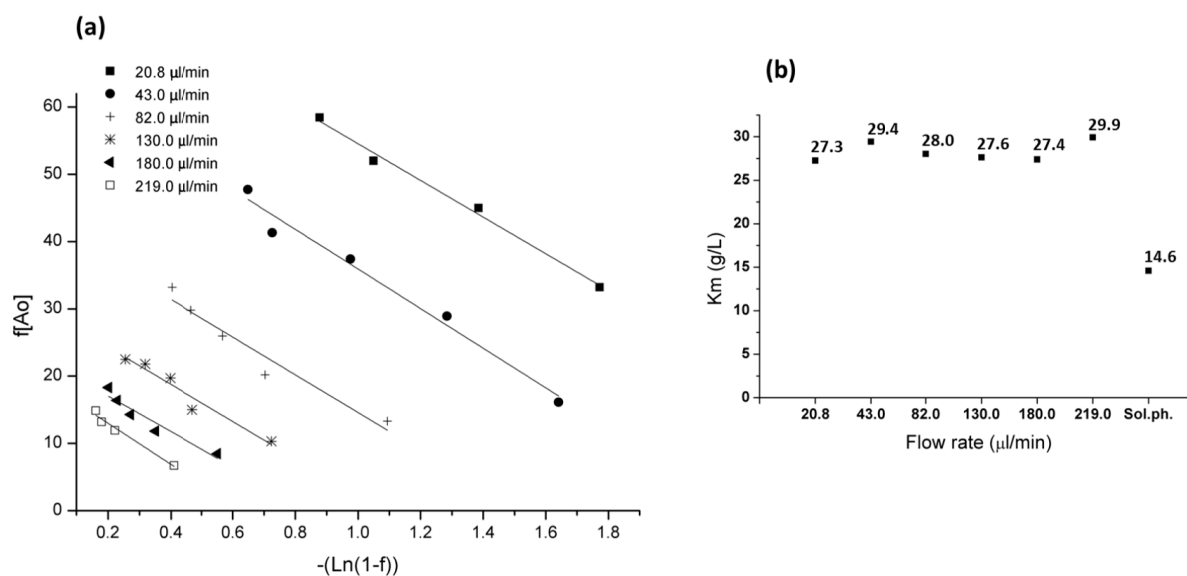


Figure 5. Determination of the Michaelis–Menten constant ($K_{m(app)}$) using the Lilly–Hornby model: (a) fitting of data to the model where the slope of the linear regression corresponds to the $K_{m(app)}$; and (b) $K_{m(app)}$ values for the immobilized invertase (average = $28.2 \pm 1.1 \text{ g}\cdot\text{L}^{-1}$) and K_m for the free invertase ($14.6 \text{ g}\cdot\text{L}^{-1}$).

2.5. Mass Transfer Effects

Further evaluation of the mass transfer effects was conducted through the determination of the Damköhler number (Da) for the several operational conditions used, viz. flow rate and substrate concentration in the range of 20.8–219.0 $\mu\text{L}\cdot\text{min}^{-1}$ and 2.0%–10.0% (w/v) respectively. The values of Reynolds number (N_{Re} , revealing that for the all conditions the flow is in the laminar regime), Sherwood number (N_{Sh}) and the liquid film mass transfer coefficient (K_L) corresponding to the flow rates applied are presented in Figure 6.

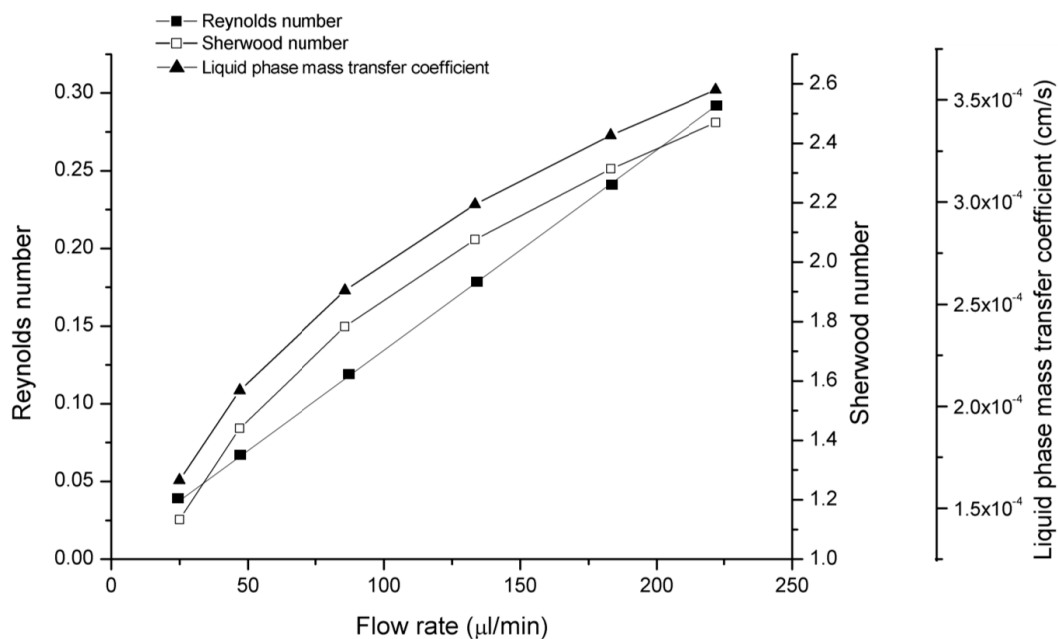


Figure 6. Determination of the Reynolds (N_{Re}) and Sherwood (N_{Sh}) number and corresponding liquid film mass transfer coefficient (K_L) values for flow rates in the range of 20.8 to 219.0 $\mu\text{L}\cdot\text{min}^{-1}$.

In Figure 7, the Da values are presented and the impact of both flow rate and substrate concentration on Da is shown.

Therefore, since substrate concentration is decreasing along the length of the reactor due to its conversion into reducing sugars, Da was calculated for the initial (Figure 7a), final (Figure 7b) and average substrate concentration (Figure 7c). All Da values are much smaller than the threshold criterion 1, indicating that under all conditions the system is being operated on the reaction rate limited regime. Moreover, as expected the highest Da values were obtained while operating the reactor at both the lowest substrate concentrations and flow rates. Increasing the value of the aforementioned conditions resulted in a noticeable decrease on the Da values. The obtained results corroborate the data attained from the Lilly–Hornby kinetic analysis. However, the kinetic model data interpretation only links the diffusional effects to the flow rates at which the reactor is being operated and lacks at describing the substrate concentration as an important driving force in molecular diffusion.

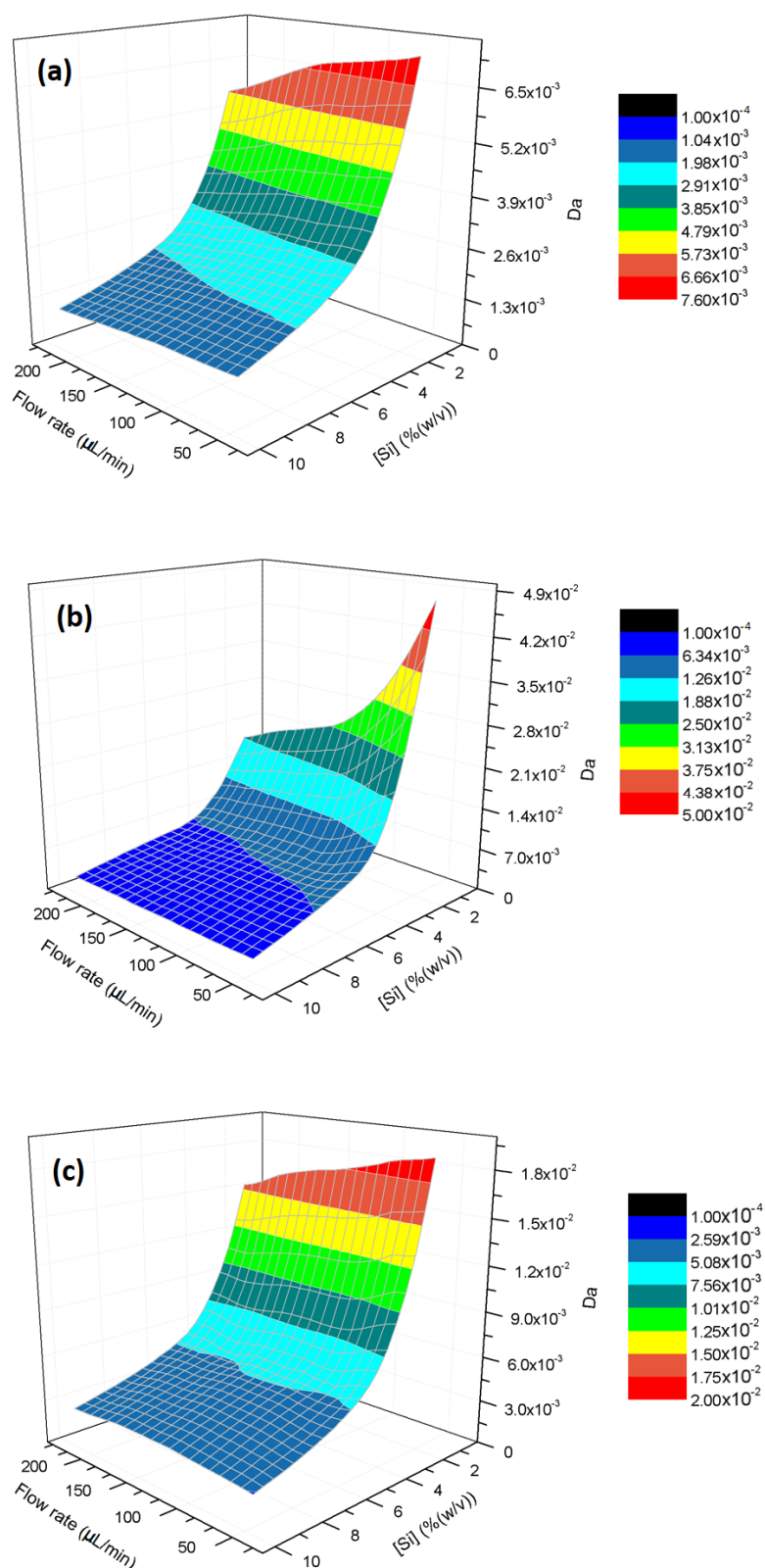


Figure 7. Damköhler numbers calculated for the operation of the microchannel reactor at flow rates and substrate concentrations in the range of 20.8–219.0 $\mu\text{L}\cdot\text{min}^{-1}$ and 2.0%–10.0% (w/v), respectively. Substrate values considered in the calculation: (a) substrate concentration at the inlet; (b) substrate concentration at the outlet; and (c) average substrate concentration.

2.6. Operational Stability on Continuous Mode

As previously mentioned, operational stability is of paramount relevance when the implementation of a biocatalytic process at the full scale is envisaged. Although this feature has been evaluated previously in recirculation mode, in immobilized enzymatic reactors continuous mode of operation is privileged. The developed microchannel reactor was continuously fed during 30 days with a 5.0% (*w/v*) sucrose solution at a flow rate of $8.0 \mu\text{L}\cdot\text{min}^{-1}$ and kept at constant temperature of $50 \text{ }^\circ\text{C}$. In these conditions, full substrate conversion was obtained. The immobilized invertase retained roughly 100% of its initial activity during 23 days decreasing to around 90% at the end of the trial (Figure 8), overall resulting in a space time yield of roughly $69.0 \text{ g}\cdot\text{L}^{-1}\cdot\text{h}^{-1}$ and a biocatalyst productivity ($\text{kg}_{\text{product}}/\text{kg}_{\text{biocatalyst}}$) of 6.32×10^5 . Furthermore, no protein was detected in the samples taken along the total time of the trial. Taking into consideration other systems for sucrose hydrolysis using immobilized invertase, space time yield compares favourably with that obtained previously under covalent binding to controlled porosity carrier ($44.82 \text{ g}\cdot\text{L}^{-1}\cdot\text{h}^{-1}$) [13], although is lower than that obtained in a polyvinyl chloride tubing in a flow-through reactor ($126 \text{ g}\cdot\text{L}^{-1}\cdot\text{h}^{-1}$) [58] and in a small fixed bed reactor (1 g catalyst) packed with active Montmorillonite K-10 particles ($200 \text{ g}\cdot\text{L}^{-1}\cdot\text{h}^{-1}$) [31]. However, in the two latter approaches, 10% and 25% of the initial activity was lost after two and four days, respectively.

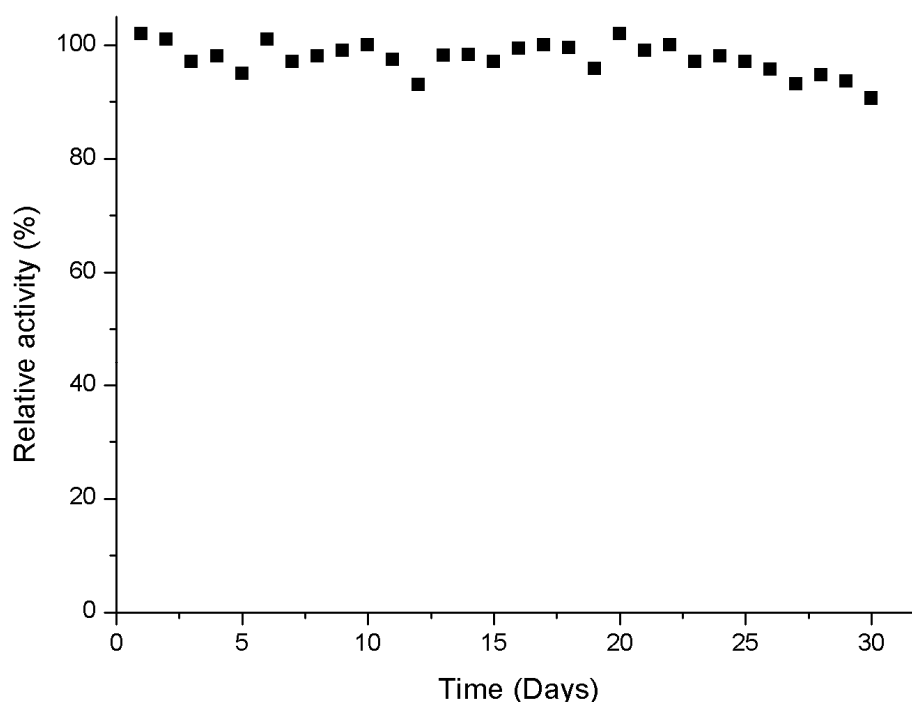


Figure 8. Operational catalytic stability of the immobilized invertase in the developed microfluidic reactor. The 5.0% (*w/v*) sucrose solution pH 4.5 was continuously fed during 30 days to the microchannel reactor at a flow rate of $8.0 \mu\text{L}\cdot\text{min}^{-1}$. Trial was performed at a constant temperature of $50 \text{ }^\circ\text{C}$. Experiments were performed in triplicates. Standard deviation did not exceed 5%.

3. Materials and Methods

3.1. Materials

Saccharomyces cerevisiae invertase (Maxinvert L 10000, batch number 611181801) was from DSM Food Specialties (Delft, The Netherlands). The 5.0 M Sodium cyanoborohydride solution, analytical grade fructose, 70.0% nitric acid and Bradford reagent were acquired from Sigma-Aldrich (Sintra, Portugal). Dipotassium hydrogen phosphate (purity $\geq 99.0\%$) and glacial acetic acid (purity $\geq 99.7\%$)

were obtained from Panreac (Cascais, Portugal). Analytical grade sucrose was acquired from Fisher Chemicals (Madrid, Spain). Sodium acetate (purity $\geq 99.0\%$) and sodium dihydrogen phosphate dihydrate (purity $\geq 98.0\%$) were purchased from VWR (Lisboa, Portugal). Pierce BCA Protein Assay Kit was acquired from Thermo Scientific (Madrid, Spain) and AT-cut piezoelectric quartz crystal sensors with a thin silicon dioxide film were obtained from Q-Sense (Valbom, Portugal).

3.2. Hydrolytic Activity of the Free Enzyme

Free enzyme trials were performed in 25 mL batch system with magnetic stirring (600 rpm) containing 10 mL of a 5.0% (*w/v*) sucrose solution prepared in 100 mM acetate buffer pH 4.5 and incubated at 50 °C. Ten microliters of invertase was used in each trial. Ten-microliter samples were collected periodically and quenched in dinitrosalicylic acid (DNS) reagent and analyzed for reducing sugars quantification. All trials were performed at least in triplicates.

3.3. Optimum pH and Temperature Determination for the Free Enzyme

Runs were performed as described in “Hydrolytic activity of the free enzyme”. The effect of pH on the hydrolytic activity of the free enzyme was assessed in the range of 3.0 to 6.0, at 50 °C. The effect of temperature was evaluated at temperatures ranging from 40 to 70 °C at pH 4.5. Values are presented in terms of relative activity and were calculated as follows:

$$\text{Relative activity (\%)} = \frac{\text{Observed activity}}{\text{maximum observed activity}} \times 100 \quad (2)$$

3.4. Free Enzyme Kinetic Parameters

Runs were performed as described in “Hydrolytic activity of the free enzyme”. Free enzyme kinetic parameters were calculated using sucrose solutions with concentrations ranging from 0.5% to 10% (*w/v*) prepared in 100 mM acetate buffer pH 4.5 at a temperature of 50 °C. Ten-microliter samples were collected until a maximum of 10% substrate conversion was achieved and the corresponding initial reaction rates were calculated. Kinetic parameters, V_{max} and K_m , were obtained through Hyper32[®] software (v1.0, University of Liverpool, Liverpool, UK, 2011).

3.5. Microchannel Reactor Assembly

Glass capillaries with 5 mm of internal diameter were heated and stretched in order to obtain thinner capillaries with internal diameter of approximately 450 μm , which were accurately selected under the microscope. An array of 40 glass capillaries (450 μm of internal diameter and 6.1 cm of length) were placed within a poly(methyl methacrylate) housing void with internal diameter of 4.0 mm and outer diameter of 6.0 mm (Figure 9). The glass capillaries and housing were glued with a methacrylate resin and incubated at room temperature for 24 h. The extremities of the assembly were capped in order to avoid capillary inner surface contamination. The obtained microchannel reactor presented a volume of approximately 390 μL and a total inner surface area of 34.5 cm^2 .

3.6. Enzyme Covalent Immobilization

Prior to reactor assembly and in order to remove surface contaminations, the capillaries were incubated in boiling nitric acid for 30 min, followed by thorough rinsing with Milli-Q water and drying with a nitrogen stream. After reactor assembly, invertase was immobilized in the inner walls of the capillaries via the APTES + glutaraldehyde methodology as described elsewhere [59]. Following immobilization, the microchannel reactor was stored at 4 °C until further use. The immobilization methodology is presented in Figure 9.

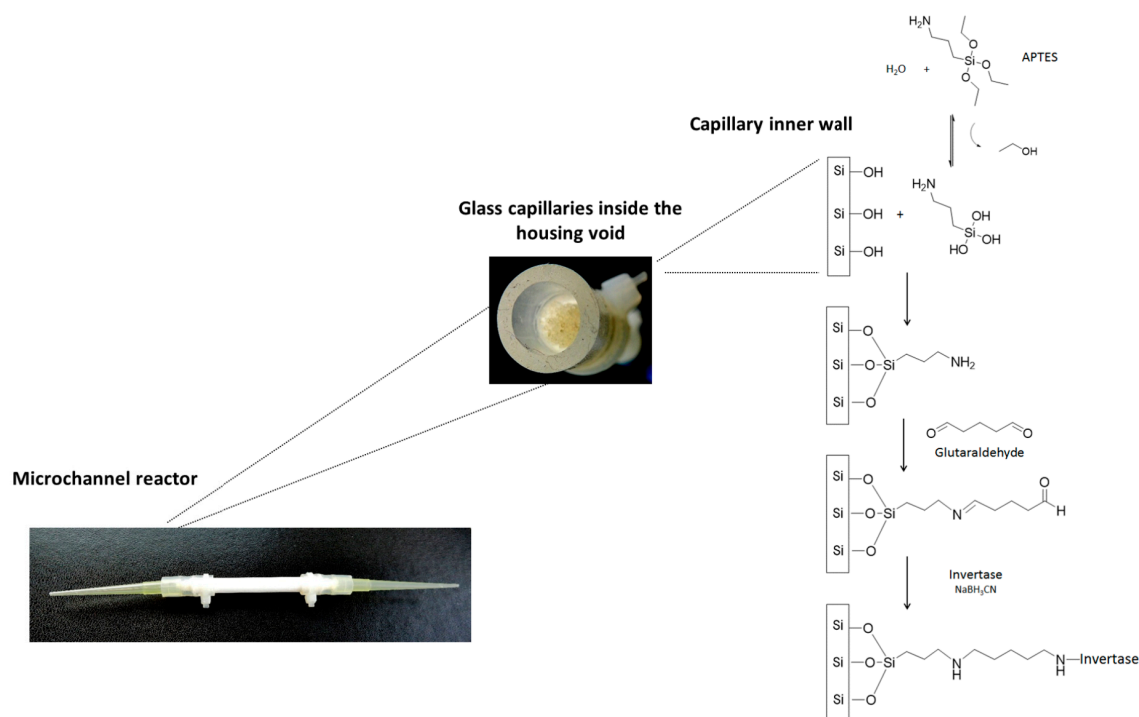


Figure 9. Microchannel reactor scheme and invertase immobilization methodology. The microchannel reactor constituted by an array of 40 glass capillaries placed within a poly(methyl methacrylate) housing void.

3.7. Hydrolytic Activity of the Immobilized Enzyme

Unless stated otherwise, 5 mL of a 5.0% (*w/v*) sucrose solution in 100 mM acetate buffer pH 4.5 were fed to the microchannel reactor in recirculation mode at a flow rate of 3.50 mL·min⁻¹ through the use of a peristaltic pump (Watson-Marlow 205 S, ERT, Lisboa, Portugal) using silicone rubber tubing (internal diameter = 1.59 mm, outer diameter = 3.18 mm and total length = 50 cm). Runs were performed at 50 °C using a temperature controlled water bath. A schematic of the set up employed is depicted in Figure 10. Samples were collected periodically and assayed for quantification of reducing sugars and protein content. All trials were performed at least in triplicates.

3.8. Microchannel Reactor Assembly and Enzyme Immobilization Reproducibility

In order to evaluate the reproducibility of both the microchannel reactor assembly and the enzyme immobilization protocol, the sucrose solution was recirculated through three reactors during 6 h. Trials were performed at pH 4.5 and at a temperature of 50 °C.

3.9. Optimum pH and Temperature Determination for the Immobilized Enzyme

The effect of temperature and pH on the hydrolytic activity of the immobilized enzyme was investigated within the same conditions used for the free enzyme. Results are presented in terms of relative activity.

3.10. Operational Stability in Recirculation Mode

In order to probe the operational stability of the immobilized invertase, four consecutive 6 h trials were performed. Experiments were carried out at pH 4.5 and at a temperature of 50 °C. After each trial the microchannel reactor was rinsed with acetate buffer 100 mM pH 4.5 and fresh substrate solution

was added. The initial reaction rate V_i for the immobilized enzyme in the microchannel reactor was calculated accordingly to Helfferich [60]:

$$V_i = \frac{v_r}{v_v} \cdot \frac{[P]}{t} \quad (3)$$

where v_r is the reaction volume, v_v is the reactor void volume, P is the product concentration and t is the time of the reaction.

3.11. Continuous Flow Operation

In the continuous flow operation mode of the developed microchannel reactor, substrate solutions were prepared in 100 mM acetate buffer pH 4.5 and fed into the reactor through the use of a peristaltic pump (Watson-Marlow 205 S, ERT, Portugal) using silicone rubber tubing (internal diameter = 1.59 mm, outer diameter = 3.18 mm). The system was kept at a constant temperature of 50 °C. The schematic of the set up employed is presented in Figure 10. Samples were collected at the outlet of the reactor once steady state was achieved and assayed for reducing sugars.

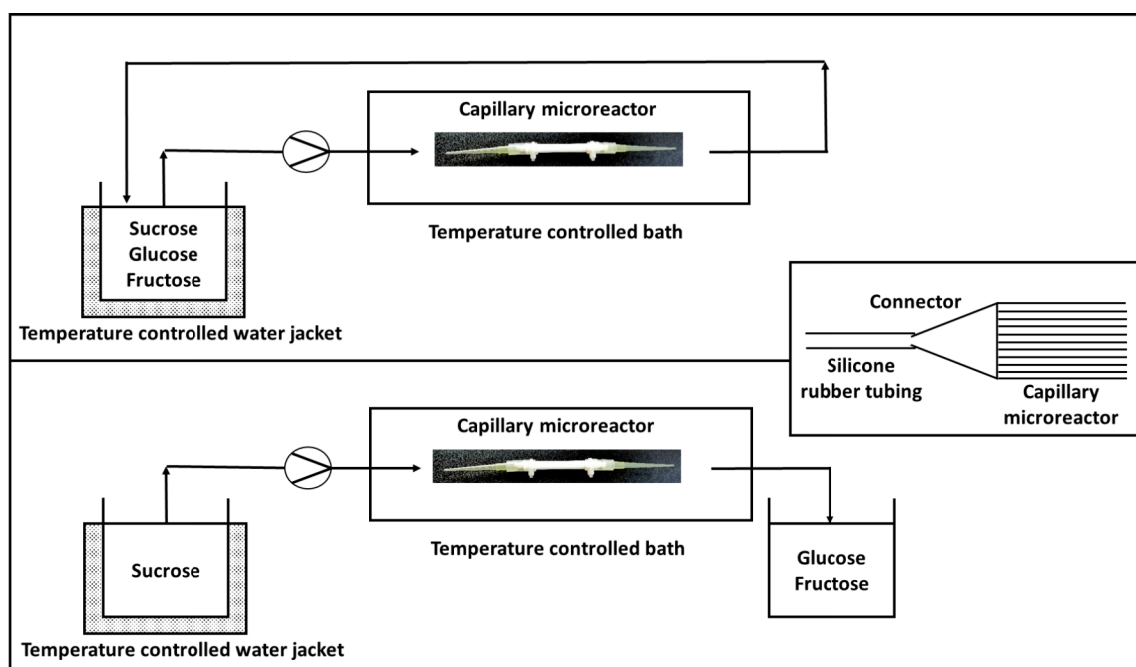


Figure 10. Schematic of the employed recirculation and continuous mode set ups. Substrate solutions were fed through the use of a peristaltic pump using silicone rubber tubing and temperature was controlled via immersion of the microchannel reactor in a water bath.

3.12. Effect of Flow Rate and Feed Concentrations on Product Yield

The effect of flow rate and feed concentration on product yield was assessed under flow rates in the range of 20.8 to 219.0 $\mu\text{L}\cdot\text{min}^{-1}$ and sucrose concentrations ranging from 2.0% to 10.0% (w/v).

3.13. Mass Transfer Effects

Mass transfer effects were assessed through the Damköhler number (Da), which establishes the ratio of the maximum reaction rate to the maximum rate of diffusion [61]:

$$Da = \frac{V_{max}}{K_L S_b} \quad (4)$$

where K_L is the liquid phase mass transfer coefficient, and S_b is the bulk substrate concentration. For values of $Da \gg 1$, the system is operating on the mass transfer limited regime, whereas, when $Da \ll 1$, the reaction rate is limiting the system. When $Da \approx 1$, the mass transfer and reaction rate are considered of comparable magnitude.

According to Carbonell et al., K_L can be expressed using the following dimensionless numbers [62]:

$$\text{Reynolds number} = N_{Re} = \frac{d_h v \rho}{\mu} \quad (5)$$

$$\text{Schmidt number} = N_{Sc} = \frac{\mu}{\rho D_s} \quad (6)$$

$$\text{Sherwood number} = N_{Sh} = 1.62 \left(\frac{d_h}{L} N_{Re} N_{Sc} \right)^{\frac{1}{3}} \quad (7)$$

where d_h is the diameter of the capillary; v is the velocity of the fluid; ρ and μ are the density and the dynamic viscosity of the fluid, respectively; L is the capillary length; and D_s is the diffusion coefficient of sucrose in water. The K_L was calculated accordingly to:

$$K_L = \frac{N_{Sh} D_s}{d_h} \quad (8)$$

3.14. Operational Stability under Continuous Flow

The operational stability of the developed microchannel reactor was evaluated during 30 days. A 5.0% (w/v) sucrose solution was continuously fed into the reactor at a flow rate of $8.0 \mu\text{L}\cdot\text{min}^{-1}$. Samples were taken on a daily basis and assayed for reducing sugar and protein content.

3.15. Analytical Methods

Quantification of the immobilized enzyme was performed through quartz crystal microbalance analysis, viz. Q-Sense E4 apparatus (Q-Sense AB, Gothenburg, Sweden), accordingly to Carvalho et al. [59]. Reducing sugar quantification was performed by the DNS method [63]. Bicinchoninic acid (BCA) method [64] was used for the quantification of the total protein present on the invertase stock solution and was used whenever reducing sugars were present.

4. Conclusions

In the present work, the development and characterization of a low cost and easy to assemble microfluidic reactor for continuous biotransformations with immobilized enzyme is reported. The microreactor was fabricated from an array of glass capillaries assembled within a poly(methyl methacrylate) housing void and invertase immobilization was carried out at the inner surface of the capillaries through the APTES + glutaraldehyde methodology. Both reactor assembly and immobilization protocol proved to be highly reproducible and similar conversion profiles were observed in microreactor replicas. Immobilization methodology did not alter significantly both the optimum catalytic pH and temperature; furthermore, it revealed to be highly robust allowing the operation of the microreactor in 4 consecutive reaction cycles while maintaining roughly the same conversion profile and initial catalytic rate.

The developed biocatalytic platform was operated in continuous mode with flow rates and substrate concentrations ranging from 20.8 to $219.0 \mu\text{L}\cdot\text{min}^{-1}$ and 2.0% – 10.0% (w/v), respectively. The immobilized enzyme presented both decreased affinity towards the substrate ($K_m = 14.6 \text{ g}\cdot\text{L}^{-1}$ and $K_{m(app)} = 28.2 \pm 1.1$) and catalytic performance (K_{cat} free enzyme = 36.6 s^{-1} and K_{cat} immobilized enzyme = 2.5 s^{-1}); moreover, the calculated $K_{m(app)}$ values showed no flow rate dependency within the range of conditions used, indicating that the system is not likely affected by mass transfer limitations.

Further evaluation of the diffusional effects was conducted through the calculation of the Damköhler number where the conclusions obtained with the kinetic model were corroborated.

Lastly, when the microreactor was operated continuously over a period of 30 days, the immobilized invertase presented remarkable operation stability, retaining roughly 100% of its initial activity during 23 days and around 90% at the end of the trial, leading to a space time yield of roughly $69.0 \text{ g}\cdot\text{L}^{-1}\cdot\text{h}^{-1}$ and a biocatalyst productivity ($kg_{\text{product}}/kg_{\text{biocatalyst}}$) of 6.32×10^5 .

The obtained results together with the low cost nature of the developed microchannel reactor clearly validate its use as a versatile tool for bioprocess development/characterization.

Acknowledgments: Filipe Carvalho acknowledges Fundação para a Ciência e a Tecnologia for PhD grant SFRH/74818/2010. Funding received by iBB-Institute for Bioengineering and Biosciences (UID/BIO/04565/2013) from the Portuguese Foundation for Science and Technology (FCT) is acknowledged.

Author Contributions: Filipe Carvalho and Pedro Fernandes conceived and designed the experiments; Filipe Carvalho performed the experiments; Filipe Carvalho, Marco P.C. Marques and Pedro Fernandes analysed the data; and Filipe Carvalho wrote the first draft of the manuscript that was then improved by Marco P.C. Marques and Pedro Fernandes.

Conflicts of Interest: The authors declare no conflict of interest.

References

1. Gomez, F.A. The future of microfluidic point-of-care diagnostic devices. *Bioanalysis* **2013**, *5*, 1–3. [[CrossRef](#)] [[PubMed](#)]
2. Jähnisch, K.; Hessel, V.; Löwe, H.; Baerns, M. Chemistry in microstructured reactors. *Angew. Chem. Int. Ed.* **2004**, *43*, 406–446. [[CrossRef](#)] [[PubMed](#)]
3. Jung, W.; Han, J.; Choi, J.-W.; Ahn, C.H. Point-of-care testing (POCT) diagnostic systems using microfluidic lab-on-a-chip technologies. *Microelectron. Eng.* **2015**, *132*, 46–57. [[CrossRef](#)]
4. Kutter, J.P. Liquid phase chromatography on microchips. *J. Chromatogr. A* **2012**, *1221*, 72–82. [[CrossRef](#)] [[PubMed](#)]
5. Nuchtavorn, N.; Suntornsuk, W.; Lunte, S.M.; Suntornsuk, L. Recent applications of microchip electrophoresis to biomedical analysis. *J. Pharm. Biomed. Anal.* **2015**, *13*, 72–96. [[CrossRef](#)] [[PubMed](#)]
6. Watts, P.; Wiles, C. Recent advances in synthetic micro reaction technology. *Chem. Commun.* **2007**, *5*, 443–467. [[CrossRef](#)] [[PubMed](#)]
7. Bolivar, J.M.; Wiesbauer, J.; Nidetzky, B. Biotransformations in microstructured reactors: More than flowing with the stream? *Trends Biotechnol.* **2011**, *29*, 333–342. [[CrossRef](#)] [[PubMed](#)]
8. Fernandes, P. Miniaturization in biocatalysis. *Int. J. Mol. Sci.* **2010**, *11*, 858–879. [[CrossRef](#)] [[PubMed](#)]
9. Marques, M.P.C.; Fernandes, P. Microfluidic devices: Useful tools for bioprocess intensification. *Molecules* **2011**, *16*, 8368–8401. [[CrossRef](#)] [[PubMed](#)]
10. Wohlgemuth, R.; Plazl, I.; Žnidaršič-Plazl, P.; Gernaey, K.V.; Woodley, J.M. Microscale technology and biocatalytic processes: Opportunities and challenges for synthesis. *Trends Biotechnol.* **2015**, *33*, 302–314. [[CrossRef](#)] [[PubMed](#)]
11. Hajba, L.; Guttman, A. Continuous-flow biochemical reactors: Biocatalysis, bioconversion, and bioanalytical applications utilizing immobilized microfluidic enzyme reactors. *J. Flow Chem.* **2016**, *6*, 8–12. [[CrossRef](#)]
12. Matosevic, S.; Lye, G.J.; Baganz, F. Immobilised enzyme microreactor for screening of multi-step bioconversions: Characterisation of a de novo transketolase- ω -transaminase pathway to synthesise chiral amino alcohols. *J. Biotechnol.* **2011**, *155*, 320–329. [[CrossRef](#)] [[PubMed](#)]
13. Carvalho, F.; Fernandes, P. Packed bed enzyme microreactor: Application in sucrose hydrolysis as proof-of-concept. *Biochem. Eng. J.* **2015**, *104*, 74–81. [[CrossRef](#)]
14. Halim, A.A.; Szita, N.; Baganz, F. Characterization and multi-step transketolase- ω -transaminase bioconversions in an immobilized enzyme microreactor (IEMR) with packed tube. *J. Biotechnol.* **2013**, *168*, 567–575. [[CrossRef](#)] [[PubMed](#)]
15. Matosevic, S.; Szita, N.; Baganz, F. Fundamentals and applications of immobilized microfluidic enzymatic reactors. *J. Chem. Technol. Biotechnol.* **2011**, *86*, 325–334. [[CrossRef](#)]
16. Stojkovič, G.; Plazl, I.; Žnidaršič-Plazl, P. L-Malic acid production within a microreactor with surface immobilised fumarase. *Microfluid. Nanofluid.* **2010**, *10*, 627–635. [[CrossRef](#)]

17. Thomsen, M.S.; Nidetzky, B. Coated-wall microreactor for continuous biocatalytic transformations using immobilized enzymes. *Biotechnol. J.* **2009**, *4*, 98–107. [[CrossRef](#)] [[PubMed](#)]
18. Sheldon, R.A. Enzyme immobilization: The quest for optimum performance. *Adv. Synth. Catal.* **2007**, *349*, 1289–1307. [[CrossRef](#)]
19. Cvjetko, M.; Vorkapić-Furač, J.; Žnidaršič-Plazl, P. Isoamyl acetate synthesis in imidazolium-based ionic liquids using packed bed enzyme microreactor. *Process Biochem.* **2012**, *47*, 1344–1350. [[CrossRef](#)]
20. Liu, J.; Lin, S.; Qi, D.; Deng, C.; Yang, P.; Zhang, X. On-chip enzymatic microreactor using trypsin-immobilized superparamagnetic nanoparticles for highly efficient proteolysis. *J. Chromatogr. A* **2007**, *1176*, 169–177. [[CrossRef](#)] [[PubMed](#)]
21. Honda, T.; Miyazaki, M.; Nakamura, H.; Maeda, H. Immobilization of enzymes on a microchannel surface through cross-linking polymerization. *Chem. Commun.* **2005**, *40*, 5062–5064. [[CrossRef](#)] [[PubMed](#)]
22. Miyazaki, M.; Kaneno, J.; Uehara, M.; Fujii, M.; Shimizu, H.; Maeda, H. Simple method for preparation of nanostructure on microchannel surface and its usage for enzyme-immobilization. *Chem. Commun.* **2003**, *5*, 648–649. [[CrossRef](#)]
23. Novick, S.J.; Rozzell, J.D. Immobilization of enzymes by covalent attachment. In *Microbial Enzymes and Biotransformations*; Barredo, J.L., Ed.; Humana Press: Totowa, NJ, USA, 2005; pp. 247–272.
24. Mohamad, N.B.; Marzuki, N.H.C.; Buang, N.A.; Huyop, F.; Wahab, R.A. An overview of technologies for immobilization of enzymes and surface analysis techniques for immobilized enzymes. *Biotechnol. Biotechnol. Equip.* **2015**, *29*, 205–220. [[CrossRef](#)] [[PubMed](#)]
25. Zhuang, W.; Zhang, Y.; He, L.; An, R.; Li, B.; Ying, H.; Wu, J.; Chen, Y.; Zhou, J.; Lu, X. Facile synthesis of amino-functionalized mesoporous TiO₂ microparticles for adenosine deaminase immobilization. *Micropor. Mesopor. Mat.* **2017**, *239*, 158–166. [[CrossRef](#)]
26. Meller, K.; Pomastowski, P.; Grzywiński, D.; Szumski, M.; Buszewski, B. Preparation and evaluation of dual-enzyme microreactor with co-immobilized trypsin and chymotrypsin. *J. Chromatogr. A* **2016**, *1440*, 45–54. [[CrossRef](#)] [[PubMed](#)]
27. Ghafourifar, G.; Waldron, K.C. Capillary electrophoretic peptide mapping to probe the immobilization/digestion conditions of glutaraldehyde-crosslinked chymotrypsin. *Curr. Anal. Chem.* **2016**, *12*, 65–73. [[CrossRef](#)]
28. Akgöl, S.; Kaçar, Y.; Denizli, A.; Arica, M. Hydrolysis of sucrose by invertase immobilized onto novel magnetic polyvinylalcohol microspheres. *Food Chem.* **2001**, *74*, 281–288. [[CrossRef](#)]
29. Azodi, M.; Falamaki, C.; Mohsenifar, A. Sucrose hydrolysis by invertase immobilized on functionalized porous silicon. *J. Mol. Catal. B: Enzymatic.* **2011**, *69*, 154–160. Available online: <http://www.sciencedirect.com/science/article/pii/S1381117711000257> (accessed on 9 January 2017). [[CrossRef](#)]
30. Kotwal, S.M.; Shankar, V. Immobilized invertase. *Biotechnol. Adv.* **2009**, *27*, 311–322. [[CrossRef](#)] [[PubMed](#)]
31. Sanjay, G.; Sugunan, S. Fixed bed reactor performance of invertase immobilized on montmorillonite. *Catal. Commun.* **2006**, *7*, 1005–1011. [[CrossRef](#)]
32. Santagapita, P.R.; Mazzobre, M.F.; Buera, P. Invertase stability in alginate beads: Effect of trehalose and chitosan inclusion and of drying methods. *Food Res. Int.* **2012**, *47*, 321–330. [[CrossRef](#)]
33. Valerio, S.G.; Alves, J.S.; Klein, M.P.; Rodrigues, R.C.; Hertz, P.F. High operational stability of invertase from *Saccharomyces cerevisiae* immobilized on chitosan nanoparticles. *Carbohydr. Polym.* **2013**, *92*, 462–468. [[CrossRef](#)] [[PubMed](#)]
34. Kulshrestha, S.; Tyagi, P.; Sindhi, V.; Yadavilli, K.S. Invertase and its applications—A brief review. *J. Pharm. Res.* **2013**, *7*, 792–797. [[CrossRef](#)]
35. Amaya-Delgado, L.; Hidalgo-Lara, M.E.; Montes-Horcasitas, M.C. Hydrolysis of sucrose by invertase immobilized on nylon-6 microbeads. *Food Chem.* **2006**, *99*, 299–304. [[CrossRef](#)]
36. Catana, R.; Eloy, M.; Rocha, J.R.; Ferreira, B.S.; Cabral, J.M.S.; Fernandes, P. Stability evaluation of an immobilized enzyme system for inulin hydrolysis. *Food Chem.* **2006**, *101*, 260–266. [[CrossRef](#)]
37. Goulart, A.J.; Francisco, A.; Tavano, O.L.; Vinueza, J.C.; Contiero, J.; Monti, R. Glucose and fructose production by *Saccharomyces cerevisiae* invertase immobilized on MANAE-agarose support. *J. Basic Appl. Pharm. Sci.* **2013**, *34*, 169–175.
38. Dehghanifard, E.; Jonidi Jafari, A.; Rezaei Kalantary, R.; Mahvi, A.H.; Faramarzi, M.A.; Esrafil, A. Biodegradation of 2,4-dinitrophenol with laccase immobilized on nano-porous silica beads. *Iranian J. Environ. Health Sci. Eng.* **2013**, *10*, 25–33. [[CrossRef](#)] [[PubMed](#)]

39. Mirzadeh, S.-S.; Khezri, S.-M.; Rezaei, S.; Forootanfar, H.; Mahvi, A.H.; Faramarzi, M.A. Decolorization of two synthetic dyes using the purified laccase of *Paraconiothyrium variabile* immobilized on porous silica beads. *J. Environ. Heal. Sci. Eng.* **2014**, *12*, 6–14. [[CrossRef](#)] [[PubMed](#)]
40. Pezzella, C.; Russo, M.E.; Marzocchella, A.; Salatino, P.; Sannia, G. Immobilization of a *Pleurotus ostreatus* laccase mixture on perlite and its application to dye decolourisation. *Biomed Res. Int.* **2014**, *2014*, 308613. [[CrossRef](#)] [[PubMed](#)]
41. Costa, S.A.; Tzanov, T.; Paar, A.; Gudelj, M.; Gübitz, G.M.; Cavaco-Paulo, A. Immobilization of catalases from *Bacillus* SF on alumina for the treatment of textile bleaching effluents. *Enzyme Microb. Technol.* **2001**, *28*, 815–819. [[CrossRef](#)]
42. Rekuć, A.; Bryjak, J.; Szymańska, K.; Jarzębski, A.B. Laccase immobilization on mesostructured cellular foams affords preparations with ultra high activity. *Process Biochem.* **2009**, *44*, 191–198. [[CrossRef](#)]
43. Anes, J.; Fernandes, P. Towards the continuous production of fructose syrups from inulin using inulinase entrapped in PVA-based particles. *Biocatal. Agric. Biotechnol.* **2014**, *3*, 296–302. [[CrossRef](#)]
44. Wilson, R.J.; Kay, G.; Lilly, M.D. The preparation and kinetics of lactate dehydrogenase attached to water-insoluble particles and sheets. *Biochem. J.* **1968**, *108*, 845–853. [[CrossRef](#)] [[PubMed](#)]
45. Cadena, P.G.; Wiggers, F.N.; Silva, R.A.; Lima Filho, J.L.; Pimentel, M.C.B. Kinetics and bioreactor studies of immobilized invertase on polyurethane rigid adhesive foam. *Bioresour. Technol.* **2011**, *102*, 513–518. [[CrossRef](#)] [[PubMed](#)]
46. Prodanović, R.; Jovanović, S.; Vujčić, Z. Immobilization of invertase on a new type of macroporous glycidyl methacrylate. *Biotechnol. Lett.* **2001**, *23*, 1171–1174. [[CrossRef](#)]
47. Kerby, M.B.; Legge, R.S.; Tripathi, A. Measurements of kinetic parameters in a microfluidic reactor. *Anal. Chem.* **2006**, *78*, 8273–8280. [[CrossRef](#)] [[PubMed](#)]
48. Lilly, M.D.; Hornby, W.E.; Crook, E.M. The kinetics of carboxymethylcellulose-ficin in packed beds. *Biochem. J.* **1966**, *100*, 718–723. [[CrossRef](#)] [[PubMed](#)]
49. Lloret, L.; Eibes, G.; Moreira, M.T.; Feijoo, G.; Lema, J.M.; Miyazakib, M. Improving the catalytic performance of laccase using a novel continuous-flow microreactor. *Chem. Eng. J.* **2013**, *223*, 497–506. [[CrossRef](#)]
50. Commenge, J.-M.; Falk, L.; Corriou, J.-P.; Matlosz, M. Analysis of microstructured reactor characteristics for process miniaturization and intensification. *Chem. Eng. Technol.* **2005**, *28*, 446–458. [[CrossRef](#)]
51. Carrara, C.R.; Mammarella, E.J.; Rubiolo, A.C. Prediction of the fixed-bed reactor behaviour using dispersion and plug-flow models with different kinetics for immobilised enzyme. *Chem. Eng. J.* **2003**, *92*, 123–129. [[CrossRef](#)]
52. Vodopivec, M.; Podgornik, A.; Berovic, M.; Strancar, A. Characterization of CIM monoliths as enzyme reactors. *J. Chromatogr. B* **2003**, *795*, 105–113. [[CrossRef](#)]
53. Seong, G.H.; Heo, J.; Crooks, R.M. Measurement of enzyme kinetics using a continuous-flow microfluidic system. *Anal. Chem.* **2003**, *75*, 3161–3167. [[CrossRef](#)] [[PubMed](#)]
54. Mao, H.; Yang, T.; Cremer, P.S. Design and characterization of immobilized enzymes in microfluidic systems. *Anal. Chem.* **2002**, *74*, 379–385. [[CrossRef](#)] [[PubMed](#)]
55. David, A.E.; Wang, N.S.; Yang, V.C.; Yang, A.J. Chemically surface modified gel (CSMG): An excellent enzyme-immobilization matrix for industrial processes. *J. Biotechnol.* **2006**, *125*, 395–407. [[CrossRef](#)] [[PubMed](#)]
56. Sabularse, V.C.; Tud, M.T.; Lacsamana, M.S.; Solivas, J.L. Black and white lahar as inorganic support for the immobilization of yeast invertase. *ASEAN J. Sci. Technol. Dev.* **2005**, *22*, 331–344. [[CrossRef](#)]
57. Uzun, K.; Çevik, E.; Şenel, M.; Baykal, A.; Abasıyanık, M.F.; Toprak, M.S. Covalent immobilization of invertase on PAMAM-dendrimer modified superparamagnetic iron oxide nanoparticles. *J. Nanopart. Res.* **2010**, *12*, 3057–3067. [[CrossRef](#)]
58. Kumar, S.; Chauhan, V.S.; Nahar, P. Invertase embedded-PVC tubing as a flow-through reactor aimed at conversion of sucrose into inverted sugar. *Enzyme Microb. Technol.* **2008**, *43*, 517–522. [[CrossRef](#)]
59. Carvalho, F.; Paradiso, P.; Saramago, B.; Ferraria, A.M.; do Rego, A.M.B.; Fernandes, P. An integrated approach for the detailed characterization of an immobilized enzyme. *J. Mol. Catal. B* **2016**, *125*, 64–74. [[CrossRef](#)]
60. Helfferich, F.G. *Kinetics of Multistep Reactions*, 2nd ed.; Elsevier: Amsterdam, The Netherlands, 2004; pp. 39–76.

61. Tibhe, J.D.; Fu, H.; Noël, T.; Wang, Q.; Meuldijk, J.; Hessel, V. Flow synthesis of phenylserine using threonine aldolase immobilized on Eupergit support. *Beilstein J. Org. Chem.* **2013**, *9*, 2168–2179. [[CrossRef](#)] [[PubMed](#)]
62. Carbonell, R.G. Mass transfer coefficients in coiled tubes. *Biotechnol. Bioeng.* **1975**, *17*, 1383–1385. [[CrossRef](#)] [[PubMed](#)]
63. Miller, G.L. Use of dinitrosalicylic acid reagent for determination of reducing sugar. *Anal. Chem.* **1959**, *31*, 426–428. [[CrossRef](#)]
64. Smith, P.K.; Krohn, R.I.; Hermanson, G.T.; Mallia, A.K.; Gartner, F.H.; Provenzano, M.D.; Fujimoto, E.K.; Goeke, N.M.; Olson, B.J.; Klenk, D.C. Measurement of protein using bicinchoninic acid. *Anal. Biochem.* **1985**, *150*, 76–85. [[CrossRef](#)]



© 2017 by the authors; licensee MDPI, Basel, Switzerland. This article is an open access article distributed under the terms and conditions of the Creative Commons Attribution (CC BY) license (<http://creativecommons.org/licenses/by/4.0/>).